Ozone air quality simulations with WRF-Chem (v3.5.1) over Europe: Model evaluation and chemical mechanism comparison

K. A. Mar[1], N. Ojha[2], A. Pozzer[2] and T. M. Butler[1]

[1]Institute for Advanced Sustainability Studies, Potsdam, Germany

[2]Atmospheric Chemistry Department, Max Planck Institute for Chemistry, Mainz, Germany

June 6, 2016

S1 Differences in implementation of dry deposition and photolysis

The MOZART mechanism in WRF uses a version of the standard WRF-Chem implementation of the Wesley dry deposition scheme (based on Wesely, 1989; Erisman et al., 1994) that has been modified to include a more complex seasonal variation in the dry deposition rates than is used in the standard implementation. Specifically, in the MOZART implementation of dry deposition, five different seasons are used to describe the variation in plant functional type, whereas in the standard implementation used by RADM2, only two seasons (summer and winter) are used. Furthermore, within the dry deposition routine, MOZART uses slightly different values for effective Henry's Law coefficients and diffusion coefficients.

As indicated in Table 2 in the main text, the scheme used to calculate photolysis rates (J values) based on radiation differs in the MOZART and RADM2 simulations. RADM2 was run with the Madronich TUV scheme, whereas MOZART chemistry in WRF is designed to run with the Madronich FTUV scheme. The FTUV model has the same physical processes as the TUV model, except that the number of wavelength bins between 121 and 750 nm are 140 for TUV vs. 17 for FTUV, which speeds up computations and leads to differences in photolysis rates of less than 5% in the troposphere, as calculated by Tie et al. (2003). An additional difference is that when MOZART is run in WRF-Chem, the standard WRF-Chem FTUV scheme is further modified to read in climatological O_3 and O_2 overhead columns rather than using a fixed value.

S2 Differences in inorganic rate coefficients

Table S1: Inorganic rate coefficients used in RADM2 that, for a July sensitivity study, were changed to match those used for the equivalent reactions in MOZART. Chemical equations and rate constant expressions are shown in the syntax of the Kinetic Pre Processor used to generate model code.

Reaction	Rate coefficient in base simulation	Rate coefficient as changed to match MOZART
O3P+NO2=NO+O2	ARR2(6.5D-12, -120.0_dp, TEMP)	ARR2(5.6e-12_dp, -180.0_dp, TEMP)
O1D+M=O3P	.78084* ARR2(1.8D-11, -110.0_dp, TEMP) + .20946e0* ARR2(3.2D-11, -70.0_dp, TEMP)	.79_dp*ARR2(2.1e-11_dp, -115.0_dp, TEMP) + .21_dp*ARR2(3.2e-11_dp, -70.0_dp, TEMP)
O3+NO=NO2+O2	ARR2(2.0D-12, 1400.0_dp, TEMP)	ARR2(3.0e-12_dp, 1500.0_dp, TEMP)
O3+OH=HO2+O2	ARR2(1.6D-12, 940.0_dp, TEMP)	ARR2(1.7e-12_dp, 940.0_dp, TEMP)
O3+HO2=OH+2.00 O2	ARR2(1.1D-14, 500.0_dp, TEMP)	ARR2(1.0e-14_dp, 490.0_dp, TEMP)
HO2+NO=NO2+OH	ARR2(3.7D-12, -240.0_dp, TEMP)	ARR2(3.5e-12_dp, -250.0_dp, TEMP)
H2O2+OH=HO2+H2O	ARR2(3.3D-12, 200.0_dp, TEMP)	ARR2(2.9e-12_dp, 160.0_dp, TEMP)
O3+NO2=NO3	ARR2(1.4D-13, 2500.0_dp, TEMP)	ARR2(1.2e-13_dp, 2450.0_dp, TEMP)
NO3+NO=NO2+NO2	ARR2(1.7D-11, -150.0_dp, TEMP)	ARR2(1.5e-11_dp, -170._dp, TEMP)
NO3+NO2=N2O5	TROE(2.20D-30 , 4.3_dp , 1.50D-12 , 0.5_dp , TEMP, C_M)	TROE(2.e-30_dp , 4.4_dp , 1.4e-12_dp , .7_dp , TEMP, C_M)
OH+NO2=HNO3	TROE(2.60D-30 , 3.2_dp , 2.40D-11 , 1.3_dp , TEMP, C_M)	TROE(2.e-30_dp , 3._dp , 2.5e-11_dp , 0._dp , TEMP, C_M)
OH+HNO3=NO3+H2O	k46(TEMP,C_M)	usr5(TEMP, C_M)
OH+HO2=H2O+O2	ARR2(4.6D-11, -230.0_dp, TEMP)	ARR2(4.8e-11_dp, -250.0_dp, TEMP)
OH+SO2=SULF+HO2	TROE(3.00D-31 , 3.3_dp , 1.50D-12 , 0.0_dp , TEMP, C_M)	usr23(TEMP, C_M)
CO+OH=HO2+CO2	(1.5D-13 * (1._dp + 2.439D-20*C_M))	usr8(temp, C_M)

Definition of rate expressions in Table S1.

```
REAL(kind=dp) FUNCTION ARR2( A0,B0, TEMP )
REAL(kind=dp) :: TEMP
REAL(kind=dp) A0,B0
ARR2 = A0 * EXP( -B0 /TEMP )
END FUNCTION ARR2

REAL(KIND=dp) FUNCTION usr5( temp, C_M )
REAL(KIND=dp), INTENT(IN) :: temp
REAL(KIND=dp), INTENT(IN) :: C_M
REAL(KIND=dp) :: k0, k2
k0 = C_M * 6.5e-34_dp * exp( 1335._dp/temp )
k2 = exp( 2199._dp/temp )
k0 = k0 /(1.0_dp + k0/(2.7e-11_dp*k2))
k2 = exp( 460._dp/temp )
usr5 = k0 + 2.4e-14_dp * k2
END FUNCTION usr5

REAL(KIND=dp) FUNCTION usr23( temp, C_M )
REAL(KIND=dp), INTENT(IN) :: temp
REAL(KIND=dp), INTENT(IN) :: C_M
REAL(KIND=dp) :: fc, k0
REAL(KIND=dp) :: wrk
fc = 3.e-11_dp * (300._dp/temp) ** 3.3_dp
wrk = fc * C_M
k0 = wrk / (1._dp + wrk/1.5e-12_dp)
usr23 = k0 * .6_dp ** (1._dp/(1._dp + (log10( wrk/1.5e-12_dp ))**2._dp))
END FUNCTION usr23

REAL(KIND=dp) FUNCTION usr8( temp, C_M )
REAL(KIND=dp), INTENT(IN) :: temp
REAL(KIND=dp), INTENT(IN) :: C_M
```

```
REAL(KIND=dp), parameter :: boltz = 1.38044e-16_dp
usr8 = 1.5e-13_dp * (1._dp + 6.e-7_dp*boltz*C_M*temp)
END FUNCTION usr8

REAL(KIND=dp) FUNCTION k46( TEMP, C_M
REAL(KIND=dp), INTENT(IN) :: temp, C_M
REAL(KIND=dp) :: k0, k2, k3
k0=7.2E-15_dp * EXP(785._dp/TEMP)
k2=4.1E-16_dp * EXP(1440._dp/TEMP)
k3=1.9E-33_dp * EXP(725._dp/TEMP) * C_M
k46=k0+k3/(1+k3/k2)
END FUNCTION k46
```

S3 Supplementary Figures

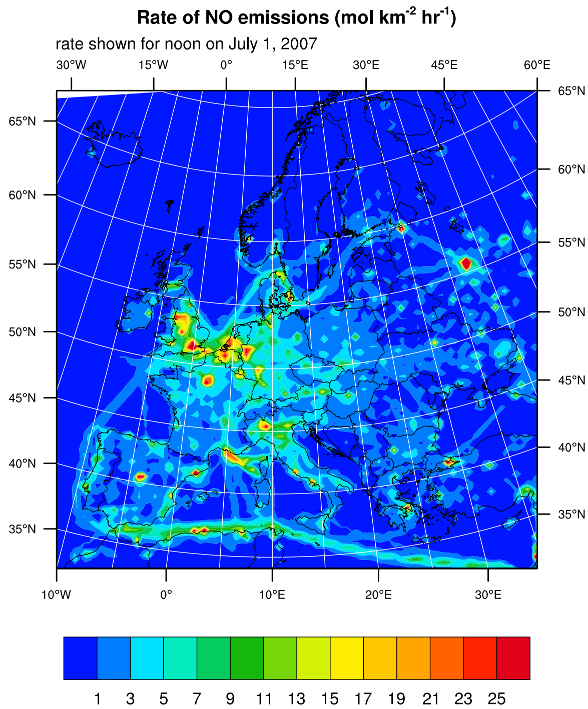

Figure S1: Example of NO emissions as processed for model input, combining the TNO-MACC II emissions inventory with the HTAP v2 inventory for the domain edges.

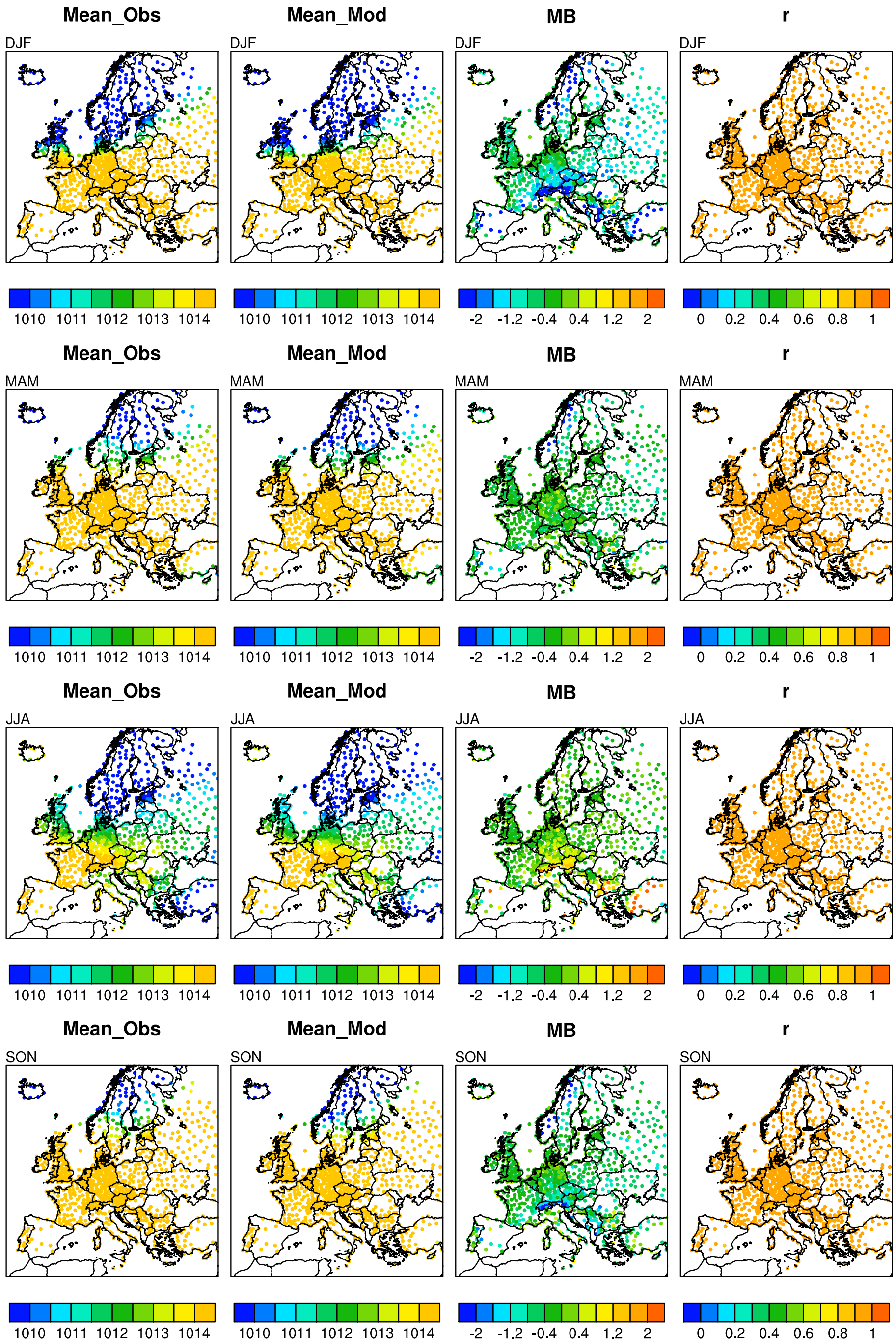

Figure S2: Seasonal average values of mean sea-level pressure (MSLP) in Pa. Model results and statistics are shown at the locations of the observations.

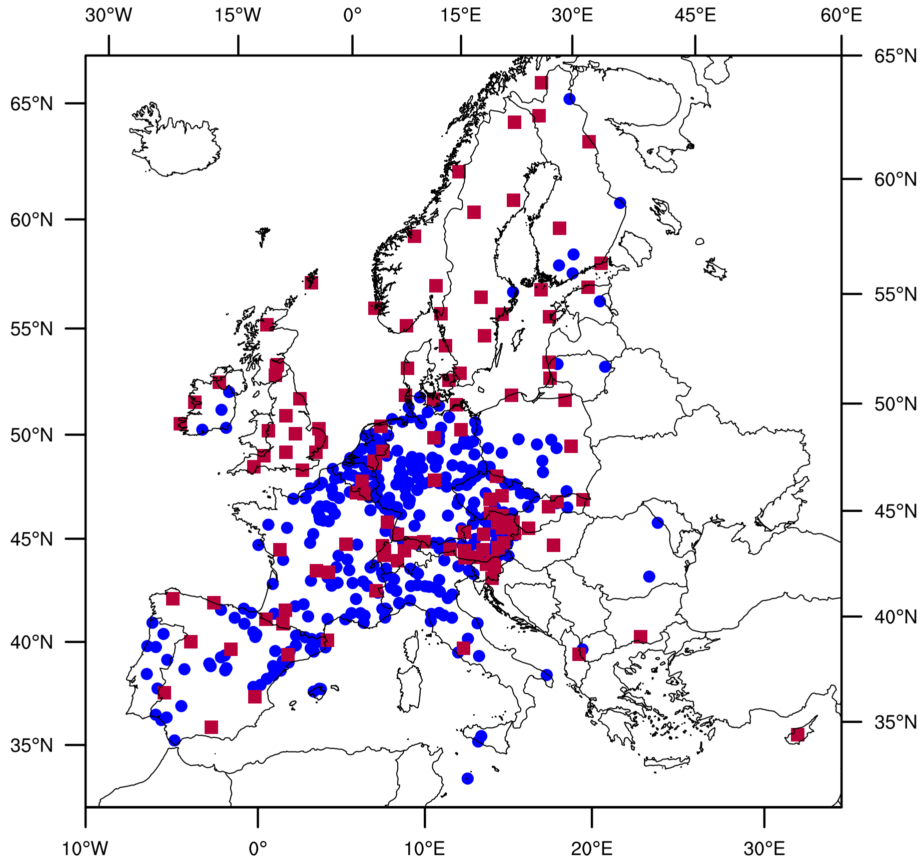

Figure S3: Location of AirBase (blue circles) and EMEP (red squares) observation sites. Shown here are stations which passed the completeness criteria for hourly O_3 measurements for summer 2007.

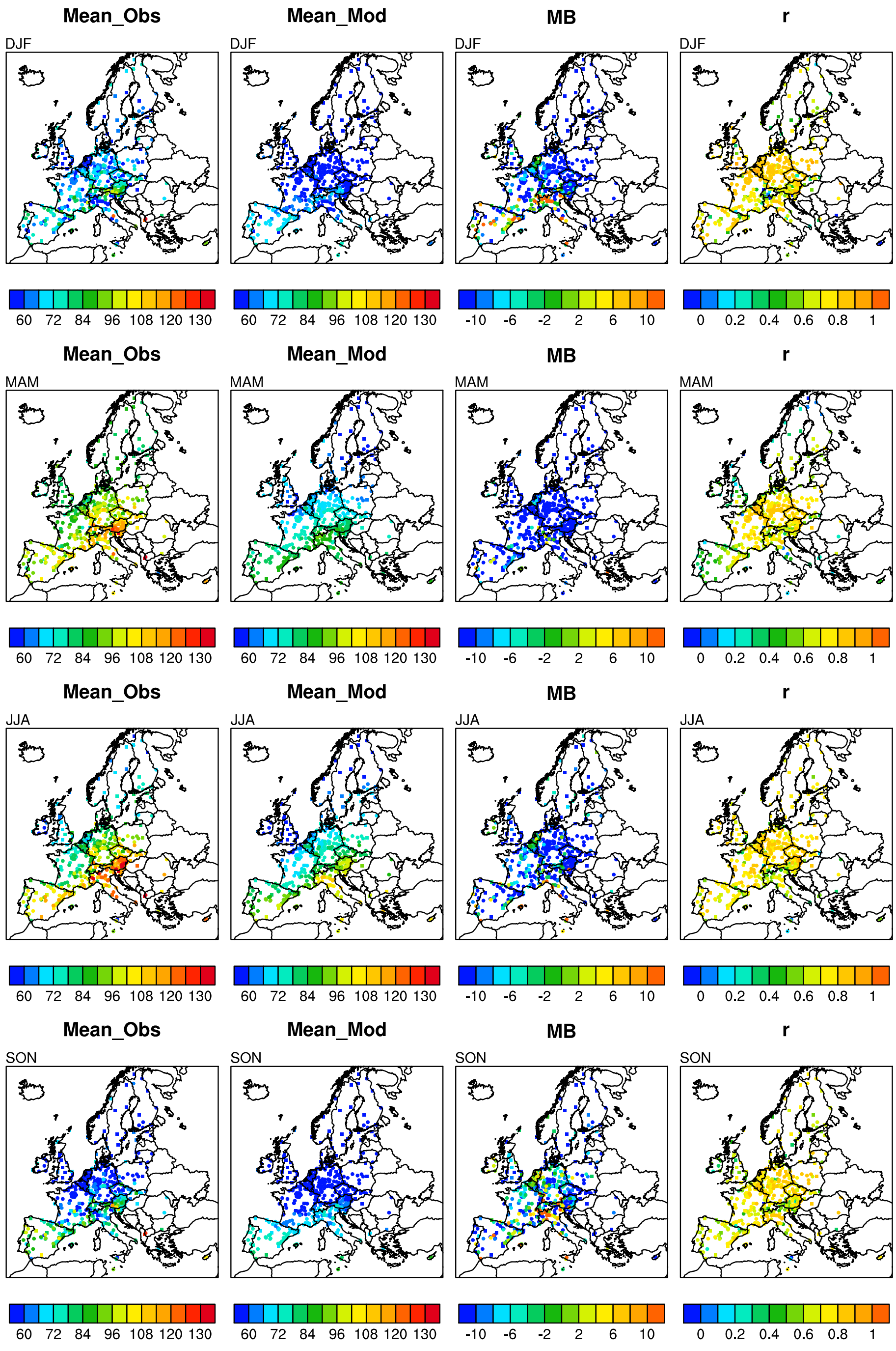

Figure S4: Seasonal average values of MDA8 in $\mu g\,m^{-3}$ calculated from hourly measurements at AirBase (circles) and EMEP (squares) stations, and modeled values from RADM2 for corresponding locations. The Mean Bias (MB, in $\mu g\,m^{-3}$) and temporal correlation coefficient (r) for daily values are also shown at the location of station observations.

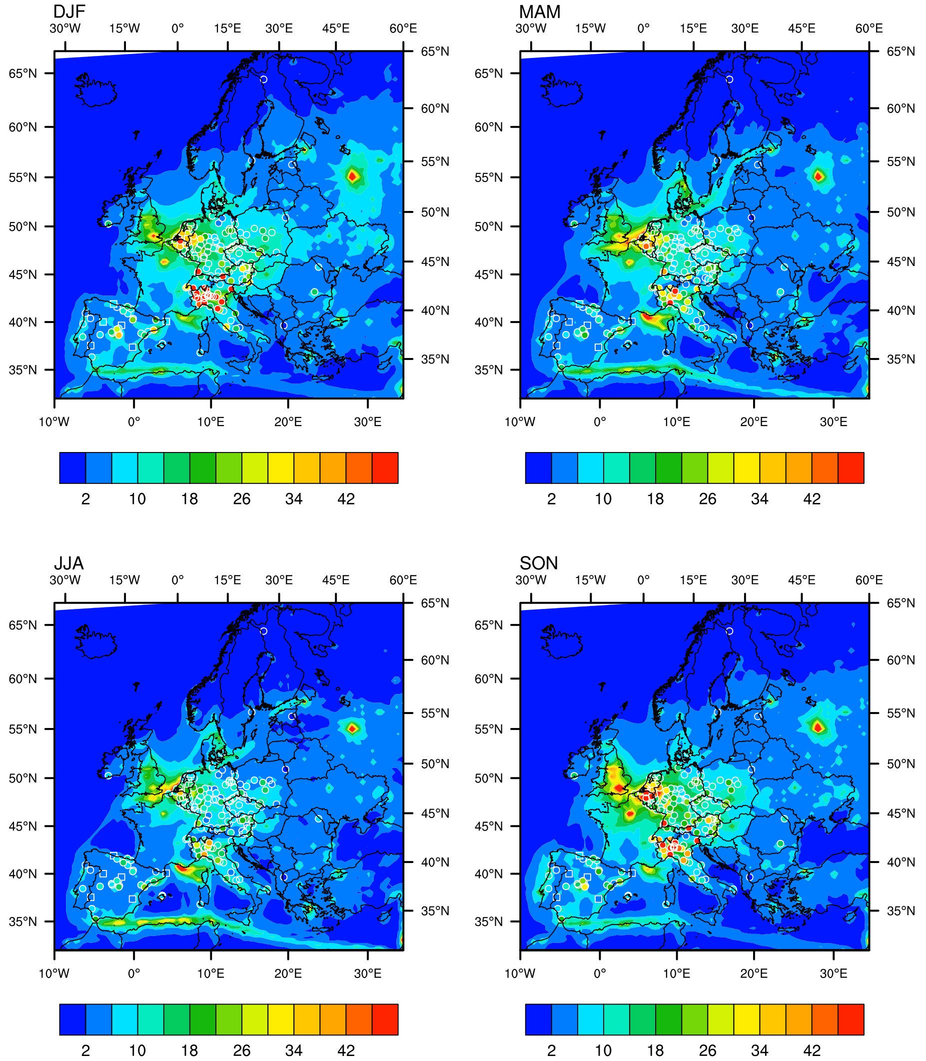

Figure S5: Seasonal average values of surface NO_x in $\mu g\,m^{-3}$. Contours are model output with the RADM2 mechanism. Filled dots represent hourly measurements at AirBase rural background stations, filled squares represent measurements at EMEP stations.

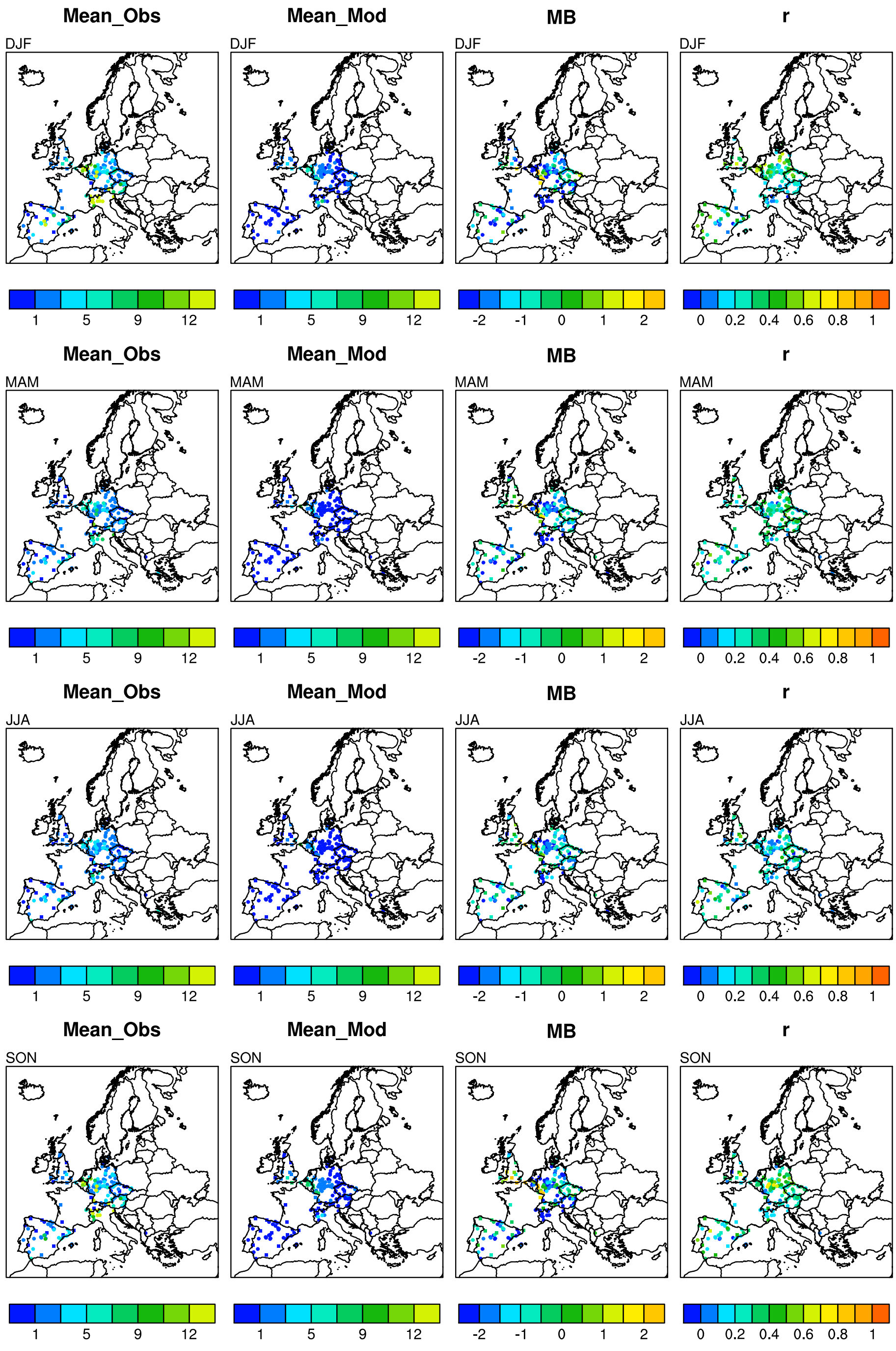

Figure S6: Seasonal average values of surface NO in $\mu g\,m^{-3}$ from hourly measurements at AirBase (circles) and EMEP (squares) stations, and modeled values from RADM2 for corresponding locations. The Mean Bias (MB) and temporal correlation coefficient (r) for hourly values are also shown at the location of station observations.

References

J. W. Erisman, A. V. Pul, and P. Wyers. Parametrization of surface resistance for the quantification of atmospheric deposition of acidifying pollutants and ozone. *Atmospheric Environment*, 28(16):2595 – 2607, 1994. ISSN 1352-2310. doi: http://dx.doi.org/10.1016/1352-2310(94)90433-2. URL http://www.sciencedirect.com/science/article/pii/1352231094904332.

X. Tie, S. Madronich, S. Walters, R. Zhang, P. Rasch, and W. Collins. Effect of clouds on photolysis and oxidants in the troposphere. *Journal of Geophysical Research: Atmospheres*, 108 (D20):n/a–n/a, 2003. ISSN 2156-2202. doi: 10.1029/2003JD003659. URL http://dx.doi.org/10.1029/2003JD003659. 4642.

M. Wesely. Parameterization of surface resistance to gaseous dry deposition in regional-scale numerical models. *Atmospheric Environment*, 23:1293–1304, 1989. doi: doi:10.1016/0004-6981(89)90153-4.